Jurnal Tribologi 16 (2018) 71-82

MYTRIBOS Malaysian Tribology Society

Jurnal Tribologi

Website : jurnaltribologi.mytribos.org e-issn: 2289-7232

Application of full factorial design to study the tribological properties of AA6061-B4C and AA6061-B4C-MoS_2 composites

Monikandan V. V. *, Joseph M. A., Rajendrakumar P. K.

Department of Mechanical Engineering, National Institute of Technology, Calicut, Kerala, INDIA.
*Corresponding author: saai.manikandan@gmail.com

KEYWORDS

MoS_2 reinforced hybrid composite
Wear studies
Full factorial design
ANOVA
Statistical analysis

ABSTRACT

This study statistically analyzes the tribological properties of AA6061-10 wt. % B4C mono composite and AA6061-10 wt.% B4C-7.5 wt. % MoS_2 hybrid composite. The tribological behavior of the composites was studied at atmospheric conditions using a pin-on-disk tribo-tester. The tribological experiments were conducted as per the full factorial design (FFD) experimental scheme. The ANOVA analysis of the wear rate revealed that the three factors, A (MoS_2 particles addition), B (applied load), and D (sliding distance) presented the physical and statistical significance on the wear rate. The ANOVA analysis of the friction coefficient revealed that the factors B (applied load) and C (sliding speed) and interaction AB (interaction of MoS_2 particles addition and applied load) presented the physical and statistical significance on the friction coefficient. It is observed from the main effects plots of the wear rate and friction coefficient that the increase in the levels of factors B (applied load) and D (sliding distance) increased the wear rate and friction coefficient. However, the wear rate and friction coefficient decreased with the increase in the level of factor A (MoS_2 particles addition).

1.0 INTRODUCTION

Particle reinforced light metal matrix composites (MMCs) are used in various commercial applications due to their low cost, high modulus and strength, high wear resistance, and processing flexibility (Lloyd, 1994). These composites are suitable for applications where the excellent tribological property is the major criterion, such as in piston rings, cylinder liners, cylinder blocks (Rohatgi, 1993), brake disk rotors, and calipers (Rohatgi, 1991). Aluminum MMCs

Received 03 Oct 2017; received in revised form 31 Oct 2017; accepted 14 Nov 2017.
To cite this article: Monikandan et al. (2018). Application of full factorial design to study the tribological properties of AA6061-B4C and AA6061-B4C-MoS_2 composites. Jurnal Tribologi 16, pp.71-82.

(AMMCs) reinforced with ceramic particles exhibited improved wear resistance when compared to the wear resistance of aluminum alloys (Prasad and Rohatgi, 1987). SiC and Al_2O_3 have been the obvious choices of reinforcement particles to fabricate the AMMCs. Studies on the tribological behavior of AMMCs reinforced with either of these conventional reinforcement particles (SiC and Al_2O_3) have frequently been reported. On the other hand, studies on AMMCs reinforced with B_4C particles are limited owing to the higher cost of the B_4C particles when compared to the cost of conventional reinforcement particles, SiC. However, it is reported that the improvement of specific properties is possible for B_4C reinforced AMMCs due to the high hardness of the B_4C particles, and the density of the B_4C is lower when compared to that of the solid aluminum (Kennedy, 2002). Hence, the investigators of this study produced an AA6061-10 wt. % B_4C mono composite and comprehensively studied its tribological properties (Monikandan et al., 2015a). Hybrid AMMCs reinforced with both the solid lubricant particles and ceramic particles exhibited anti-seizure and wear resistance properties. It is reported that in the dry environment, the MoS_2 exhibited far superior lubricating characteristics when compared to that of the Gr (graphite) (Prasad and Asthana, 2004).

Several studies reported the influence of MoS_2 particles on the tribological behavior of composites reinforced with MoS_2 particles. Formation of MoS_2-rich transfer layer on the worn surfaces of Ag-Cu-MoS_2 composites which slid against Ag-Cu counterface, reduced the wear loss and friction coefficient of the composites (Zhang et al., 2012). In the case of Cu-MoS_2 and Cu-$MoSe_2$ composites that slid against Cu counterface the solid lubrication became significant when the respective concentration of the MoS_2 or $MoSe_2$ particles increased beyond 5 wt. % (Kovalchenko et al., 2012). It is observed that the Fe-Cu-C-MoS_2 composites exhibited better tribological characteristics due to the addition of MoS_2 particles up to 3 vol. %. However, the tribological characteristics started to degrade when the concentration of MoS2 particles increased beyond 3 vol. % up to 5 vol. % (Dhanasekaran and Gnanamoorthy, 2007). The tribological properties of Al-Al2O3-MoS2 hybrid composites are statistically analyzed, and it is observed that the specific wear rate and friction coefficient are significantly influenced by the addition of MoS_2 particles (Dharmalingam et al., 2011). The abrasive wear behavior of Al-$Al2O_3$-MoS_2 hybrid composites is statistically analyzed, and it is reported that the wear rate and friction coefficient decreased with the increase in the addition of MoS_2 particles (Dharmalingam et al., 2013). The statistical studies on the tribological behavior of hybrid AMMCs reinforced with Gr particles revealed the concentration of Gr as a statistically significant factor that influenced the wear loss (Ravindran et al., 2012; Monikandan et al., 2015b). The statistical analysis of wear behavior of Al-SiC-Gr hybrid composites revealed that the % of Gr addition, sliding speed, applied load, and sliding distance influenced the wear. Interactions are also observed among the factors, sliding speed, applied load, and sliding distance (Suresha and Sridhara, 2010a). In related work, the same authors statistically analyzed the friction characteristics of Al-SiC-Gr hybrid composites and observed that the friction coefficient is influenced by sliding speed and applied load (Suresha and Sridhara, 2012).

Literature makes it clear that the tribo-test parameters and the concentration of solid lubricant particles influence the tribological behavior of the hybrid composites. The tribological studies of hybrid composites reinforced with B_4C particles as ceramic phase are limited. Further, studies on statistical analysis of the tribological behavior of Al-B_4C-MoS_2 hybrid composites are lacking. Hence, in the present study, the tribological behavior of AA6061-10 wt. % B_4C mono composite and the AA6061-10 wt. % B_4C-7.5 wt. % MoS_2 hybrid composite is statistically analyzed to understand the statistical significance of different tribo-test parameters and MoS_2 particles addition on the wear rate and friction coefficient. The better self-lubricating properties of the Al-

B_4C-MoS_2 hybrid composites make them potential substitutes for Al-Si alloys and composites that are presently used to fabricate different automotive components. It is to be noted that the authors of this study had extensively studied the dry sliding tribological behavior of AA6061-B_4C-Gr and AA6061-B_4C-MoS_2 hybrid composites (Monikandan et al., 2016a; Monikandan et al., 2016b). Before conducting the extensive studies on the tribological behavior of these hybrid composites, statistical analysis was carried out as per the experimental scheme designed using full factorial design (FFD) to identify the factors (reinforcement particles, applied load, sliding speed, and sliding distance) and interaction of factors that significantly influence the tribological behavior. In an earlier work, the investigators of this study statistically analyzed the tribological properties of AA6061-B_4C-Gr hybrid composite (Monikandan et al., 2015b). In the present work, the results of the statistical analysis of tribological properties of AA6061-B_4C-MoS_2 composite are reported.

2.0 MATERIALS

The AA6061-10 wt. % B_4C mono composite is fabricated using stir casting, and the stir casting procedure is explained in an earlier work together with the XRD spectrum and micrographs (Monikandan et al., 2015a). The stir casting method used to fabricate the AA6061-10 wt. % B_4C-7.5 wt. % MoS_2 hybrid composite is explained in previous work (Monikandan et al., 2016b). The XRD spectrum and metallograph of the hybrid composite are also available in the same work.

3.0 EXPERIMENTATION SCHEME AND TRIBO-TESTS

The tribo-tests are conducted as per the full factorial experimental scheme. This scheme and the conditions and details of the tribo-tests are discussed in the following sections.

3.1 Experimentation scheme

The tribological experiments are carried out as per the FFD experimental scheme. Minitab 17 (Minitab Inc.) statistical software was used for this purpose. The MoS_2 particles addition (factor A), applied load (factor B), sliding speed (factor C), and sliding distance (factor D) were varied for two levels of 0 and 7.5 wt. %, 10 and 50 N, 0.5 and 2.5 m/s, and 200 and 1000 m, respectively. The four factors (A, B, C, and D) were varied for two levels which constitute 2^4 FFD. The selection of high level of factor A is determined by the wt. % addition of MoS_2 particles. It is to be noted that the composites are cast using in-house stir casting facility. The maximum amount of MoS_2 particles that can be added to the melt without sedimentation of MoS_2 particles is 7.5 wt. %. Hence, the addition of MoS_2 particles (factor A) is limited to 7.5 wt. %. In the case of solid lubricant reinforced hybrid composites, usually, low applied load and sliding speed are conducive for the formation of solid lubricant-rich tribolayer while high applied load and sliding speed demoted its formation (Riahi and Alpas, 2001). This phenomenon, in turn, influences the tribological properties of the solid lubricant reinforced hybrid composites. Hence, in this study, 10 and 50 N are selected as the low and high levels of applied load, respectively and 0.5 and 2.5 m/s are selected as the low and high levels of sliding speed, respectively. It is reported that the friction coefficient of Al-B_4C composite varied significantly within 1000 m sliding distance (Shorowordi et al., 2006). Furthermore, we observed that the wear rate and friction coefficient of Al-B_4C composite varied considerably within the short sliding distance range of 200 to 1000 m (Monikandan, 2015a). Hence, in this study, the low and high levels of sliding distance are selected

as 200 and 1000 m, respectively. The factors and their levels are tabulated in Table 1. The track radius was kept constant throughout the tests (150 mm).

Table 1: Factors and levels of 24 FFD scheme.

S. No	Factors	Naming conventions used	Low level	High level
1	MoS_2 particles (wt. %)	A	0	7.5
2	Applied load (N)	B	10	50
3	Sliding speed (m/s)	C	0.5	2.5
4	Sliding distance (m)	D	200	1000

It is reported that the FFD scheme is beneficial in the early stages of the experimental study, particularly if the number of factors of the study is less than or equal to four. Also, this design helps to understand the preliminary trend of the responses. The experimental combinations of the FFD were randomized to avoid the uncontrolled factors from following any specific pattern.

3.2 Tribo-tests

Dry sliding wear tests were performed on a pin-on-disc tribo-tester (Ducom, TR-20 LE) as per ASTM G99-05 Standard. The tests were conducted under atmospheric conditions (1 atm., 30 ± 1 ˚C, and 70 ± 5 % RH) against the EN 31 bearing steel disk (C-0.99, Mn-0.35, Si-0.25, P-0.025, S-0.025, Cr-1.40, Mo-0.1, Ni-0.25, Cu-0.35, and the balance Fe by wt. %). The hardness and surface roughness of the disk were measured to be 65 HRC and 0.1 μm, respectively. Before each test, the pin surface was polished rough using 600 grit abrasive sheet. The finely polished pin surface is likely to carry protruded B_4C particles which induce micro-cutting on the counterface at the beginning of the sliding. The wear loss was measured using a precision weighing balance of sensitivity, 0.1 mg. The wear rate was obtained using the formula $W=\delta W/S$ where W is the wear rate in mg/m; δW is the weight difference of the pin before and after the test in mg and S is the sliding distance in m. The coefficient of friction was computed as the ratio of tangential friction force to the applied normal force. The tests were repeated three times to confirm the repeatability of the readings and the average of the three readings were used for the statistical analysis of tribological properties.

4.0 RESULTS AND DISCUSSION

The responses (wear rate and friction coefficient) obtained by performing the wear tests as per the experimental scheme are tabulated in Table 2. The experimental readings (responses) were analyzed using analysis of variance (ANOVA) technique which helps to draw important inferences (Ravindran et al., 2012).

ANOVA is used when the design scheme has more than one factor or two levels. ANOVA is used to observe the effect of factors and the effect of interaction of factors on the responses (Pannerselvam, 2012). Tables 3 and 4 show the ANOVA of the wear rate and friction coefficient, respectively. The level of significance (α) was selected as 0.05. Both tables (Table 3 and 4) show the standard error of the regression (S), R-Squared (R-Sq), Adjusted R-Squared (R-Sq (adj)), source, degree of freedom (DF), sequential sum of squares (Seq SS), adjusted sum of squares (Adj SS), adjusted mean squares (Adj MS), F-ratio (F), P-value (P), and percentage of contribution P

(%). The percentage of contribution was calculated with the formula, P (%) = (Seq SS_F/Seq SS_T) x 100 where Seq SS_F is the sequential sum of squares of the factors or the interactions and Seq SS_T is the total sum of squares. The factors and interactions having the higher P (%) value than the P (%) value of error is considered as statistically and physically significant (Toptan et al., 2012).

It is observed from Table 3 that the P (%) value of the factors A (6.75 %), B (20.94 %), and D (63.51 %) are higher than the P (%) value of the error (4.72 %). The P (%) value of factor C and the P (%) value of all the interactions are lower than the P (%) value of the error. Hence, the factors A, B, and D presented the statistical and physical significance on the wear rate. Factor C and all the interactions are not statistically and physically significant to influence the wear rate. Further, the factor D that has the highest P (%) value of 63.51 % provided the strongest statistical and physical significance on the wear rate. In the case of friction coefficient, Table 4 shows that the P (%) value of factors B (26.39 %) and C (21.91 %) and interaction of factors AB (21.30 %) are higher than the P (%) value of the error (8.84 %). Meanwhile, the P (%) value of factor D and all the other interaction of factors are less than the P (%) value of error. Hence, it is evident that the factors B and C and the interaction of factors AB presented the statistical and physical significance on the friction coefficient. Further, the factor B with the highest P (%) value of 26.39 % provided the strongest statistical and physical significance on the friction coefficient. The ANOVA of the wear rate revealed that the parameters of the tribo-tests (factors B and D) and the MoS2 particles addition (factor A) presented statistical and physical significance on the wear rate. The ANOVA of the friction coefficient revealed that the factors B and C and interaction of factors AB presented statistical and physical significance on the friction coefficient.

Table 2: Experimental scheme and responses.

A (wt. %)	**B (N)**	**C (m/s)**	**D (m)**	**Wear rate (mg/m)**	**Friction coefficient**
7.5	10	0.5	200	0.00317	0.409
0.0	50	2.5	200	0.00567	0.412
0.0	10	0.5	200	0.00433	0.401
0.0	10	0.5	1000	0.00767	0.418
0.0	10	2.5	200	0.00350	0.332
7.5	50	0.5	1000	0.00900	0.449
0.0	50	2.5	1000	0.01183	0.448
7.5	10	2.5	1000	0.00500	0.416
7.5	50	2.5	1000	0.01017	0.392
0.0	10	2.5	1000	0.00883	0.404
7.5	10	0.5	1000	0.00833	0.413
7.5	50	2.5	200	0.00550	0.403
7.5	10	2.5	200	0.00233	0.409
7.5	50	0.5	200	0.00433	0.419
0.0	50	0.5	1000	0.01283	0.487
0.0	50	0.5	200	0.00600	0.507

Table 3: ANOVA of wear rate.

Source	DF	Seq SS	Adj SS	Adj MS	F	P	P (%)
A	1	0.1E-4	0.1E-4	0.1E-4	7.11	0.045	6.75
B	1	0.31E-4	0.31E-4	0.31E-4	21.24	0.006	20.94
C	1	0.1E-5	0.1E-5	0.1E-5	0.35	0.582	0.67
D	1	0.94E-4	0.94E-4	0.94E-4	65.15	0	63.51
AB	1	0	0	0	0.14	0.719	0
AC	1	0	0	0	0.03	0.870	0
AD	1	0.1E-5	0.1E-5	0.1E-5	0.87	0.393	0.67
BC	1	0.1E-5	0.1E-5	0.1E-5	1.02	0.360	0.67
BD	1	0.2E-5	0.2E-5	0.2E-5	1.47	0.280	1.35
CD	1	0	0	0	0.06	0.818	0
Error	5	0.7E-5	0.7E-5	0.1E-5			4.72
Total	15	0.148E-3					
		S = 0.0012027, R-sq = 95.12 % and R-Sq (adj) = 85.36 %					

Table 4: ANOVA of friction coefficient.

Source	DF	Seq SS	Adj SS	Adj MS	F	P	P (%)
A	1	0.000613	0.000613	0.000613	1.47	0.279	2.60
B	1	0.006202	0.006202	0.006202	14.92	0.012	26.39
C	1	0.005148	0.005148	0.005148	12.38	0.017	21.91
D	1	0.001139	0.001139	0.001139	2.74	0.159	4.84
AB	1	0.005006	0.005006	0.005006	12.04	0.018	21.30
AC	1	0.001351	0.001351	0.001351	3.25	0.131	5.75
AD	1	0.000352	0.000352	0.000352	0.85	0.400	1.49
BC	1	0.001008	0.001008	0.001008	2.42	0.180	4.29
BD	1	0.000264	0.000264	0.000264	0.64	0.462	1.12
CD	1	0.000333	0.000333	0.000333	0.80	0.412	1.41
Error	5	0.002079	0.002079	0.000416			8.84
Total	15	0.023493					
		S = 0.0203903, R-Sq = 91.15 % and R-Sq (adj) = 73.45 %					

Figure 1(a) and (b) shows the normal effects plots of the wear rate and friction coefficient, respectively and the plots also demonstrate the direction of the effect too. It is inferred from Figure 1(a) that the factors B and D lie on the right side of the normal probability line and as these factors increased from low to high level, the wear rate increased. Meanwhile, factor A lies on the left side of the normal probability line, and as this factor increased from low to high level, the wear rate decreased. The statistical analysis of wear characteristics of Al-SiC-Gr hybrid composites revealed the similar phenomenon (Suresha and Sridhara, 2010b).

In the case of friction coefficient, factor B lies on the right side of the normal probability line (Figure 1(b)), and as this factor increased from low to high level, the friction coefficient increased.

However, factor C lies on the left side of the normal probability line, and as this factor increased from low to high level, the friction coefficient decreased. In the case of wear rate, factor D exhibited the largest standardized effect, and for friction coefficient, factor B exhibited the largest standardized effect. Also, it is observed from Figure 1(a) that the factors A, B, and D statistically influenced the wear rate and it is observed from Figure 1(b) that the factors B and C and interaction of factors AB statistically influenced the friction coefficient.

The normal probability plots of the wear rate and friction coefficient are shown in Figure 2(a) and (b), respectively. The residual points seem to be on a straight line which suggests that they follow a normal distribution (Mathews, 2005) and, no outlier is observed on the plots. Further, no change of slope of the normal probability line is observed, indicating that there are no factors other than the ones considered in the experimental study influence the tribological properties of the composites. The main effects plots are used to depict the effect of the tribo-test parameters and particles addition on the wear rate and friction coefficient (Suresha and Sridhara, 2010c).

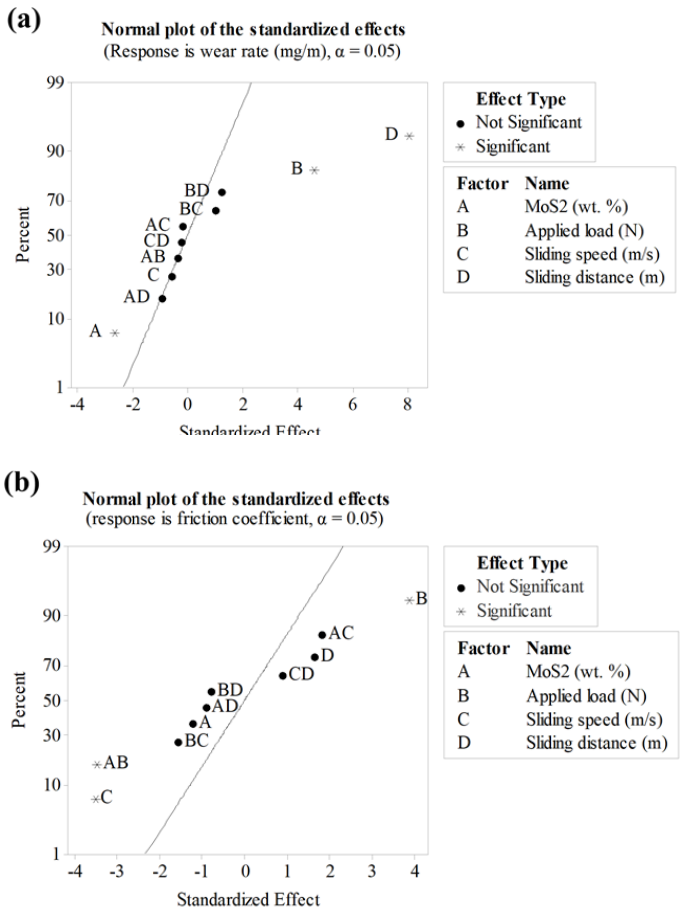

Figure 1: Normal effects plots (a) Wear rate and (b) friction coefficient.

It is observed from Figure 3(a) that the wear rate increased as the factors B and D increased from 10 to 50 N and 200 to 1000 m, respectively. It is observed from Figure 3(b) that the increase in sliding speed (factor C) from 0.5 to 2.5 m/s reduced the friction coefficient. It is to be noted that the metal dichalcogenide, MoS_2 is a solid lubricant. The addition of MoS_2 particles (factor A) led to the formation of MoS_2-rich tribolayer which provided solid lubrication and hence, the wear rate and friction coefficient decreased. It is reported that the presence of solid lubricants such as MoS_2 (Zhang et al., 2012), graphite (Hirai et al., 2016), graphene (Kumar and Wani, 2017), or hexagonal boron nitride (Mushtaq and Wani, 2017) on the contact surfaces led to the better tribological properties. Figure 4 shows the SEM micrograph of MoS_2-rich tribolayer formed on the 7.5 wt. % MoS_2 hybrid composite worn pin surface. The smeared MoS_2 particles of the tribolayer are marked with an arrow, and the smeared AA6061 matrix material debris is indicated with the dotted arrow, and the oxidized iron particles are indicated using an open arrow. The iron particles are transferred from the EN 31 counterface during the formation of the MoS_2-rich tribolayer.

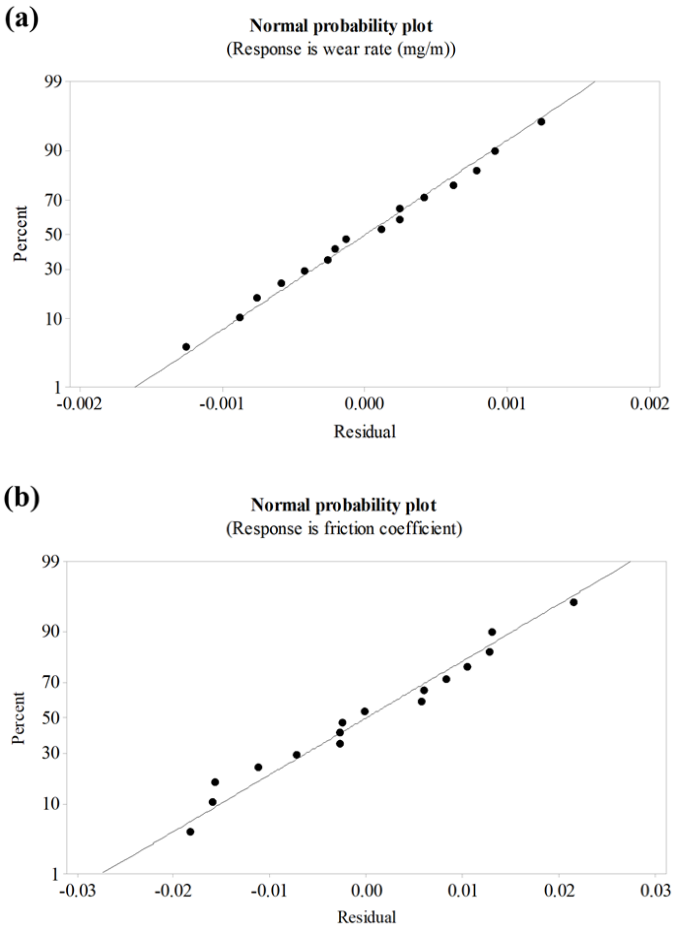

Figure 2: Normal probability plots (a) Wear rate and (b) friction coefficient.

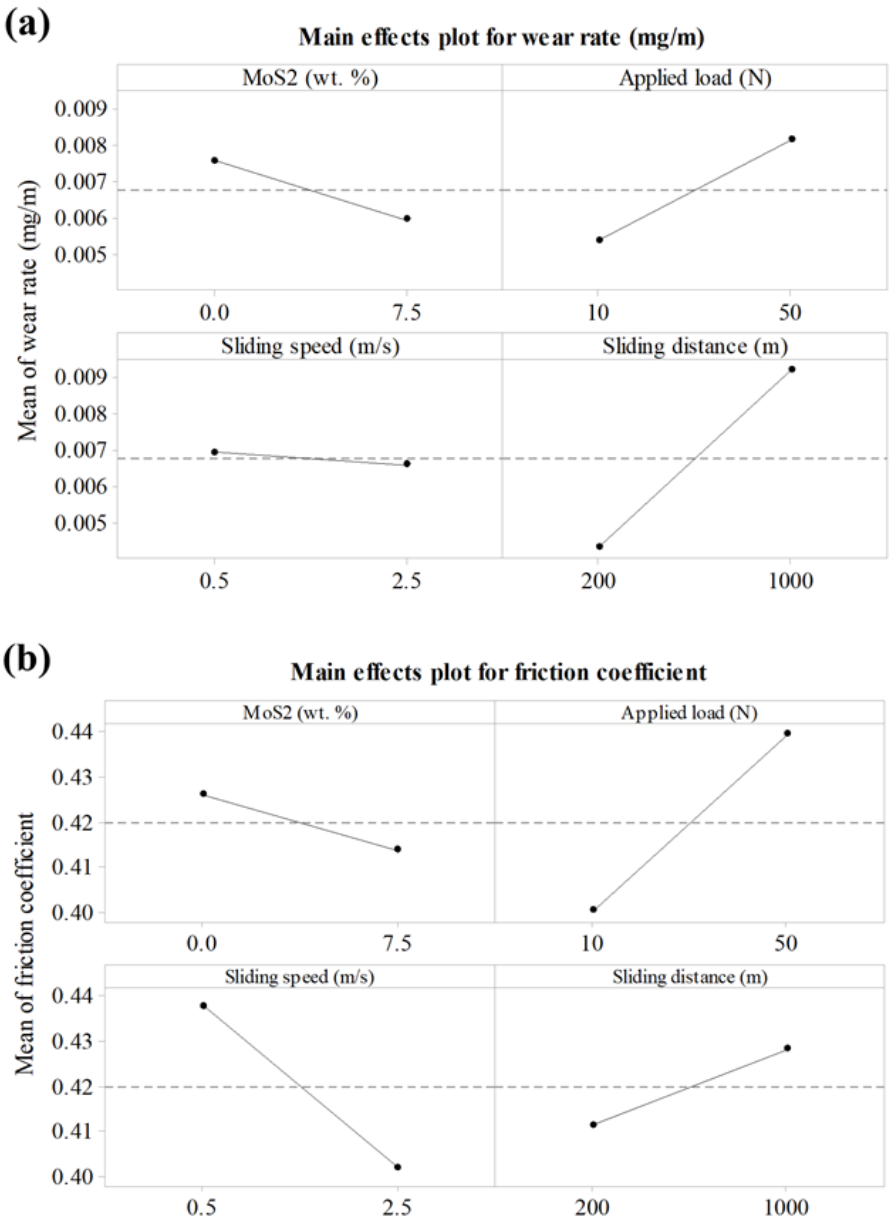

Figure 3: Main effects plots (a) Wear rate and (b) friction coefficient.

It is observed from the normal effects plot of friction coefficient (Figure 1(b)) that interaction exists between the factors A and B. The interaction between the factors A and B is graphically illustrated using the interaction plot as shown in Figure 5. The interaction plot shows the interaction between factors and the effect of interaction of factors on the response (Saini et al., 2012). The friction coefficient increased with increase in applied load (factor B) for both the mono and hybrid composites. However, in the case of hybrid composites, the MoS_2 particles (factor A) reduced the degree of increase of the friction coefficient. Hence, factor A also influenced the

response. This phenomenon (Influence of the factors A and B on the friction coefficient) is suggestive of the interaction between the factors A and B. Also, the continuous and dotted lines which represent the mean friction coefficient of the mono and hybrid composites respectively, are not parallel to each other. This non-parallelism between the continuous and dotted lines also indicated the interaction between the factors A and B.

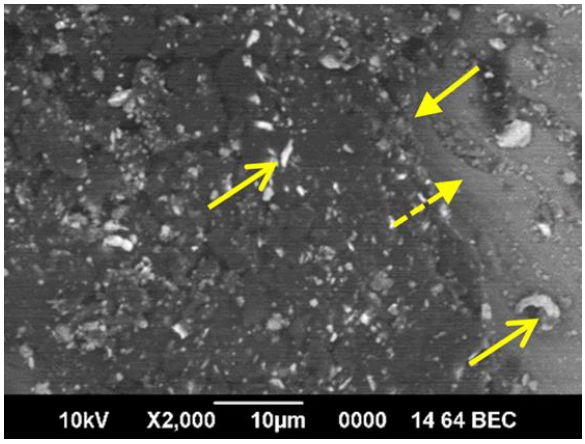

Figure 4: BSE micrograph showing smeared MoS_2 particles (marked with arrow), smeared matrix material debris (marked with dotted arrow), and the oxidized iron particles (marked with open arrow) (sliding speed 0.5 m/s, applied load 10 N, and sliding distance 200 m).

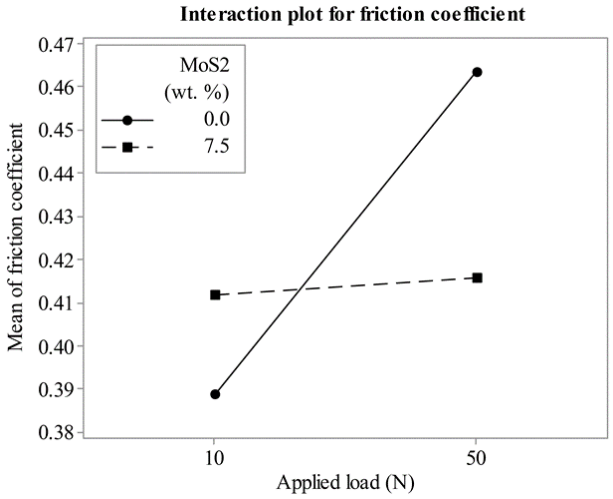

Figure 5: Interaction plot of friction coefficient.

5.0 CONCLUSION

The statistical analysis of the tribological properties of AA6061-10 wt. % B_4C mono composite and AA6061-10 wt. % B_4C-7.5 wt. % MoS_2 hybrid composite have been carried out using factors, (i) MoS_2 particles addition (0 and 7.5 wt. %), (ii) applied load (10 and 50 N), (iii) sliding speed

(0.5 and 2.5 m/s), and (iv) sliding distance (200 and 1000 m). The following are the crucial inferences of the statistical analysis:

a) The ANOVA analysis of the wear rate revealed that the factors A (MoS_2 particles addition), B (applied load), and D (sliding distance) presented physical and statistical significance on the wear rate. The ANOVA analysis of the friction coefficient revealed that the factors B (applied load) and C (sliding speed) and interaction of factors AB (interaction of MoS_2 particles addition and applied load) presented the physical and statistical significance on the friction coefficient.
b) The normal probability plots of the wear rate and friction coefficient revealed the absence of outliers and no change in slope of the normal probability line confirmed that all the relevant factors that influenced the tribological properties of the composites were included in the experimental scheme.
c) The main effects plots of the wear rate and friction coefficient revealed that as the factors B (applied load) and D (sliding distance) increased from their low to high level, the wear rate and friction coefficient increased. On the contrary, when factor A (MoS_2 particles addition) increased from low to high level, the wear rate and friction coefficient decreased.
d) In the case of friction coefficient, statistically and physically significant interaction existed among the factors A (MoS_2 particles addition) and B (applied load) as revealed by the interaction plot.

REFERENCES

Dhanasekaran, S., & Gnanamoorthy, R. (2007). Abrasive wear behavior of sintered steels prepared with MoS_2 addition. Wear, 262(5-6), 617-623.

Dharmalingam, S., Subramanian, R., & Kök, M. (2013). Optimization of abrasive wear performance in aluminium hybrid metal matrix composites using Taguchi–grey relational analysis. Proceedings of the Institution of Mechanical Engineers, Part J: Journal of Engineering Tribology, 227(7), 749-760.

Dharmalingam, S., Subramanian, R., Vinoth, K. S., & Anandavel, B. (2011). Optimization of tribological properties in aluminum hybrid metal matrix composites using gray-Taguchi method. Journal of Materials Engineering and Performance, 20(8), 1457-1466.

Hirai, Y., Sato, T., & Usami, H. (2016). Combined effects of graphite and sulfide on the tribological properties of bronze under dry conditions. Jurnal Tribologi, 11, 14-23.

Kennedy, A. R. (2002). The microstructure and mechanical properties of Al-Si-B4C metal matrix composites. Journal of Materials Science, 37(2), 317-323.

Kovalchenko, A. M., Fushchich, O. I., & Danyluk, S. (2012). The tribological properties and mechanism of wear of Cu-based sintered powder materials containing molybdenum disulfide and molybdenum diselenite under unlubricated sliding against copper. Wear, 290, 106-123.

Kumar, P., & Wani, M. F. (2017). Synthesis and tribological properties of graphene: A review. Jurnal Tribologi, 13, 36-71.

Lloyd, D. J. (1994). Particle reinforced aluminium and magnesium matrix composites. International materials reviews, 39(1), 1-23.

Mathews, P. G. (2005). Design of Experiments with MINITAB. ASQ Quality Press.

Monikandan, V. V., Joseph, M. A., & Rajendrakumar, P. K. (2016a). Dry Sliding Tribological Studies of AA6061-B4C-Gr Hybrid Composites. Journal of Materials Engineering and Performance, 25(10), 4219-4229.

Monikandan, V. V., Joseph, M. A., & Rajendrakumar, P. K. (2016b). Dry sliding wear studies of aluminum matrix hybrid composites. Resource-Efficient Technologies, 2, S12-S24.

Monikandan, V. V., Joseph, M. A., Rajendrakumar, P. K., & Sreejith, M. (2015a). Tribological behavior of liquid metallurgy-processed AA 6061-B4C composites. Materials Research Express, 2(1), 1-11.

Monikandan, V. V., Jacob, J. C., Joseph, M. A., & Rajendrakumar, P. K. (2015b). Statistical analysis of tribological properties of aluminum matrix composites using full factorial design. Transactions of the Indian Institute of Metals, 68(1), 53-57.

Mushtaq, S., & Wani, M. F. (2017). Self-lubricating tribological characterization of lead free Fe-Cu based plain bearing material. Jurnal Tribologi, 12, 18-37.

Pannerselvam, R. (2012). Design and analysis of experiments. PHI Learning Pvt. Ltd.

Prasad, S. V., & Asthana, R. (2004). Aluminum metal-matrix composites for automotive applications: Tribological considerations. Tribology letters, 17(3), 445-453.

Prasad, S. V., & Rohatgi, P. K. (1987). Tribological properties of Al alloy particle composites. JOM, 39(11), 22-26.

Ravindran, P., Manisekar, K., Narayanasamy, P., Selvakumar, N., & Narayanasamy, R. (2012). Application of factorial techniques to study the wear of Al hybrid composites with graphite addition. Materials & Design, 39, 42-54.

Riahi, A. R., & Alpas, A. T. (2001). The role of tribo-layers on the sliding wear behavior of graphitic aluminum matrix composites. Wear, 251(1-12), 1396-1407.

Rohatgi, P. K. (1991). Cast aluminum-matrix composites for automotive applications. JOM, 43(4), 10-15.

Rohatgi, P. K. (1993). Metal matrix composites. Defence Science Journal, 43(4), 323-349.

Saini, S., Ahuja, I. S., & Sharma, V. S. (2012). Influence of cutting parameters on tool wear and surface roughness in hard turning of AISI H11 tool steel using ceramic tools. International Journal of Precision Engineering and Manufacturing, 13(8), 1295-1302.

Shorowordi, K. M., Haseeb, A. S. M. A., & Celis, J. P. (2006). Tribo-surface characteristics of Al–B4C and Al–SiC composites worn under different contact pressures. Wear, 261(5-6), 634-641.

Suresha, S., & Sridhara, B. K. (2010a). Effect of addition of graphite particulates on the wear behaviour in aluminium–silicon carbide–graphite composites. Materials & Design, 31(4), 1804-1812.

Suresha, S., & Sridhara, B. K. (2010b). Wear characteristics of hybrid aluminium matrix composites reinforced with graphite and silicon carbide particulates. Composites Science and Technology, 70(11), 1652-1659.

Suresha, S., & Sridhara, B. K. (2010c). Effect of silicon carbide particulates on wear resistance of graphitic aluminium matrix composites. Materials & Design, 31(9), 4470-4477.

Suresha, S., & Sridhara, B. K. (2012). Friction characteristics of aluminium silicon carbide graphite hybrid composites. Materials & Design, 34, 576-583.

Toptan, F., Kerti, I., & Rocha, L. A. (2012). Reciprocal dry sliding wear behaviour of B4Cp reinforced aluminium alloy matrix composites. Wear, 290, 74-85.

Zhang, L., Xiao, J., & Zhou, K. (2012). Sliding wear behavior of silver–molybdenum disulfide composite. Tribology Transactions, 55(4), 473-480.